Energy-Efficient Beaconless Geographic Routing in Wireless Sensor Networks

Haibo Zhang and Hong Shen

Abstract—Geographic routing is an attractive localized routing scheme for wireless sensor networks (WSNs) due to its desirable scalability and efficiency. Maintaining neighborhood information for packet forwarding can achieve a high efficiency in geographic routing, but may not be appropriate for WSNs in highly dynamic scenarios where network topology changes frequently due to nodes mobility and availability. We propose a novel online routing scheme, called Energy-efficient Beaconless Geographic Routing (EBGR), which can provide loop-free, fully stateless, energy-efficient sensor-to-sink routing at a low communication overhead without the help of prior neighborhood knowledge. In EBGR, each node first calculates its ideal next-hop relay position on the straight line toward the sink based on the energy-optimal forwarding distance, and each forwarder selects the neighbor closest to its ideal next-hop relay position as the next-hop relay using the Request-To-Send/Clear-To-Send (RTS/CTS) handshaking mechanism. We establish the lower and upper bounds on hop count and the upper bound on energy consumption under EBGR for sensor-to-sink routing, assuming no packet loss and no failures in greedy forwarding. Moreover, we demonstrate that the expected total energy consumption along a route toward the sink under EBGR approaches to the lower bound with the increase of node deployment density. We also extend EBGR to lossy sensor networks to provide energy-efficient routing in the presence of unreliable communication links. Simulation results show that our scheme significantly outperforms existing protocols in wireless sensor networks with highly dynamic network topologies.

Index Terms—Wireless sensor networks, beaconless geographic routing, power-aware routing, energy-efficient.

1 Introduction

Geographic routing, in which each node forwards packets only based on the locations of itself, its directed neighbors, and the destination, is particularly attractive to resource-constrained sensor networks. The localized nature of geographic routing eliminates the overhead brought by route establishment and maintenance, indicating the advantages of modest memory requirement at each node and high scalability in large distributed applications. In conventional geographic routing schemes, each node is required to maintain more or less accurate position information of all its direct neighbors, and the position of a node is made available to its direct neighbors by periodically broadcasting beacons. In WSNs with invariant or slowly changing network topology, maintaining neighbor information can greatly improve the performance because of the reusability of the maintained information and the low maintenance cost. However, in many application scenarios, WSNs are highly dynamic and the network topology may frequently change due to node mobility, node sleeping [16], [20], node or link faults, etc. In highly dynamic scenarios, routing protocols based on maintaining neighbor information suffer from at least three drawbacks. First, the maintenance of neighbor information causes too much communication overhead and results in significant energy expenditure. Second, the collected neighbor information can quickly get outdated, which, in turn, leads to frequent packet drops. Third, the maintenance of neighbor information consumes memory which is also a scarce resource in WSNs.

To overcome the drawbacks of conventional geographic routing schemes in scenarios with dynamic network topology, several beaconless geographic routing protocols [15], [12], [5], [9], [17], [35] have been proposed. Beaconless routing schemes, in which each node forwards packets without the help of beacons and without the maintenance of neighbor information, are fully reactive. When a node has a packet to transmit, it broadcasts the packet to its neighbors. The most suitable neighbor for further relaying the packet is determined based on a contention mechanism in which each neighbor determines a proper delay for further forwarding the packet based on how well it is suited as the next-hop relay. Therefore, beaconless routing schemes are robust to topology changes since the forwarding decision is based on the actual topology at the time a packet is to be forwarded. However, in most existing beaconless routing schemes such as BLR [15], CBF [12], and GDBF [9], each node forwards packets based on hop-count routing metrics (e.g., each node selects its neighbor closest to the destination as its next-hop relay). These routing metrics are simple in implementation, but they cannot guarantee energy efficiency which is a major concern in WSNs.

In this paper, we address the problem of providing energy-efficient beaconless geographic routing for dynamic wireless sensor networks in which network topology frequently changes over time, and present a novel routing protocol called Energy-efficient Beaconless Geographic Routing (EBGR). Without any prior knowledge of neighbors, EBGR tries to minimize the total energy consumed by

- *H. Zhang is with the Automatic Control Laboratory, Royal Institute of Technology, Stockholm, Sweden. E-mail: haibo@kth.se.*
- *H. Shen is with the School of Computer Science, The University of Adelaide, SA 5005, Australia. E-mail: hong@cs.adelaide.edu.au.*

Manuscript received 21 Oct. 2008; revised 19 May 2009; accepted 29 May 2009; published online 12 June 2009.
Recommended for acceptance by P. Mohapatra.
For information on obtaining reprints of this article, please send e-mail to: tpds@computer.org, and reference IEEECS Log Number TPDS-2008-10-0425.
Digital Object Identifier no. 10.1109/TPDS.2009.98.

delivering each packet to the sink and works as follows: each sensor node first calculates its ideal next-hop relay position based on the optimal forwarding distance in terms of minimizing the total energy consumption for delivering a packet to the sink. When a node has a packet to transmit, it first broadcasts an RTS message to detect its best next-hop relay. All suitable neighbors in the relay search region participate in the next-hop relay selection process using a timer-based contention mechanism. Each candidate that receives the RTS message sets a delay for broadcasting a corresponding CTS message based on a discrete delay function, which guarantees that the neighbor closest to the optimal relay position has the shortest delay. The neighbor that has the minimum delay broadcasts its CTS message first, and the other candidates snooping the CTS message notice that another node has responded the request and quit the contention process. Finally, the packet is unicasted to the established next-hop relay. If there is no node in the relay search region, the forwarding node enters into a beaconless recovery mode to recover from the local minimum. The key contributions of this paper are summarized as follows:

- We propose a novel online geographic routing scheme called EBGR, which can provide fully stateless, energy-efficient sensor-to-sink routing at a low communication overhead without maintaining neighborhood information.
- We prove that EBGR is loop-free in greedy forwarding mode, and establish the lower and upper bounds on hop count for sensor-to-sink routing in uniform sensor networks, assuming no failures in greedy forwarding.
- We establish the upper bound on energy consumption for sensor-to-sink data delivery under EBGR, assuming no packet loss and no failures in greedy forwarding mode.
- We extend EBGR to handle the unreliable communication links which are common in realistic applications of WSNs.
- We evaluate the performance of EBGR in three scenarios: mobility, random sleeping, and high-variant link quality. Simulation results show that our scheme significantly outperforms existing routing protocols in highly dynamic scenarios.

The rest of this paper is structured as follows: The related work on power-aware routing and geographic routing is discussed in Section 2. The system models are described in Section 3. The energy-efficient beaconless geographic routing protocol EBGR is presented in Section 4. In Section 5, we give extensive theoretical analysis for EBGR. In Section 6, we extend EBGR to lossy wireless sensor networks. In Section 7, we evaluate our scheme through extensive simulations and present the comparisons with other protocols. Finally, we conclude the paper and discuss future extensions in Section 8.

2 Related Work

Wireless communication is a major source of energy consumption in WSNs. Thus, it is essential to design energy-aware routing schemes to improve energy efficiency. In the past few decades, energy-aware routing has received much attention in wireless ad hoc/sensor networks. Singh et al. [28] introduced the concept of energy-aware routing and proposed five metrics, i.e., *minimize energy consumed/packet, maximize time to network partition, minimize variance in node power levels, minimize cost/packet,* and *minimize maximum node cost,* for routing in mobile ad hoc networks. Stojmenovic and Lin [31] discussed the importance of designing localized power-aware routing protocols for WSNs and proposed three fully localized routing algorithms to minimize total energy consumption. A framework based on optimizing *cost over progress ratio* was further proposed in [29] for designing energy-aware routing schemes in wireless networks. The objective of improving energy efficiency is to extend network lifetime. Routing algorithms aiming at maximizing network lifetime have also been designed in [8], [18], [31].

Geographic routing makes routing decisions only based on the locations of a node's one-hop neighbors, thereby avoiding the overhead of maintaining global topology information. The MFR protocol proposed in [32] is one of the earliest geographic routing algorithms in which each node forwards its packets to the neighbor that has the maximum progress. In *"greedy" routing* [10], each node forwards the packets to its neighbor closest to the destination. However, these schemes cannot guarantee that packets are delivered in an energy-efficient manner. Recently, some work has been done on improving energy efficiency for geographic routing. In [33], a protocol called GPER was proposed to provide power-efficient geographic routing in WSNs. In [24], a novel analytical framework was introduced to analyze the relationship between energy efficiency and range of topology knowledge. Routing metrics based on normalized advance have been designed in [21], [22]. Based on a realistic physical layer model, the $PRR \times DIST$ routing metric was first introduced in [21] to deal with the unreliable communication in wireless ad hoc networks. PRR is the packet reception rate and DIST is the transmission distance. In $PRR \times DIST$ routing metric, each node selects the neighbor with the largest $PRR \times DIST$ as the next-hop relay. In [27], Seada et al. addressed the *weak-link* problem and studied the energy and reliability tradeoffs pertaining to geographic forwarding in lossy sensor networks using the $PRR \times DIST$ metric.

To deal with the dynamic network topology, beaconless routing, in which each node forwards packets without maintaining neighbor information, has been proposed. In [15], Heissenbuttel et al. proposed the Beacon-Less Routing (BLR) algorithm. In BLR, optimized forwarding is achieved by applying a concept of Dynamic Forwarding Delay (DFD). In contention-based forwarding (CBF) [12], Füßler et al. proposed a technique called *active selection method* in which a forwarding node selects its next-hop relay through broadcasting control message. The implicit geographic forwarding (IGF) proposed by Blum et al. [5] and the geographic random forwarding (GeRaF) proposed by Zorzi [36] implement the same ideas but focus on the integration of beaconless routing with the IEEE 802.11 MAC layer. However, most of the proposed beaconless schemes employ

hop-count-based routing metric, which is not efficient in terms of energy consumption. A beaconless routing algorithm which uses a cost-over-progress approach to determine energy-optimal links was proposed in [13].

Most geographic routing protocols use greedy forwarding as the basic mode of operation. Greedy forwarding may fail when a node cannot find a better neighbor than itself to forward the packet. To recover from a local minimum, GFG [25], GPSR [6], and GOAFR+ [19] route a packet around the faces of a planar subgraph (e.g., *Relative Neighborhood Graph* (RNG) and *Gabriel Graph* (GG)) when a local minimum is encountered. However, the planar subgraphs are constructed based on neighborhood information which is not a prior knowledge in beaconless routing schemes. In BLR [15], a *Request-response* approach was proposed for recovering from local minima. In [17], algorithms for constructing different proximity graphs in beaconless routing were designed. Two schemes, Beaconless Forwarder Planarization (BFP) and Angular Relaying, were proposed. To provide guaranteed delivery in WSNs, most existing geographic routing algorithms [2], [25], [11], [15], [17] switch between the greedy forwarding mode and recovery mode depending on the network topology.

3 Preliminaries

3.1 Network Model

Without loss of generality, it is assumed that no two nodes locate at the same position. All sensor nodes are equipped with the same radio transceiver that enables a maximum transmission range R. Each node knows its own location as well as the location of the sink. We use the *Unit Disk Graph (UDG)* communication model in the first stage of analysis. In this model, any two nodes u and v can communicate with each other reliably if and only if $|uv| \leq R$, where $|uv|$ is the euclidean distance between u and v. In Section 6, based on a realistic communication model in which data loss is estimated by packets reception rate, we extend our scheme to achieve localized energy-efficient beaconless routing in the presence of unreliable communication links.

3.2 Energy Model

The *First Order Radio Model* proposed in [14] has been widely used for measuring energy consumption in wireless communications [4], [23], [24], [31], [33]. In this model, the energy for transmitting 1 bit data over distance x is $\epsilon_t(x) = a_{11} + a_2 x^k$, where a_{11} is the energy spent by transmitter electronics, a_2 is the transmitting amplifier, and $k (k \geq 2)$ is the propagation loss exponent. The energy for receiving 1 bit data is $\epsilon_r = a_{12}$, where a_{12} is the energy spent by receiver electronics. Therefore, the energy consumed by relaying 1 bit data (i.e., receiving 1 bit data, and then, transmitting it over distance x) is

$$\varepsilon_{relay}(x) = a_{11} + a_2 x^k + a_{12} \equiv a_1 + a_2 x^k, \quad (1)$$

where $a_1 = a_{11} + a_{12}$.

3.3 Characteristics of Power-Adjusted Transmission

In [30], the characteristics of energy consumption for power adjusted transmission were investigated using a generalized form of the *First Order Radio Model*. Given a source node u and a destination node v, d denotes the distance between u and v, and $\xi(d)$ represents the total energy consumed by delivering 1 bit data from u to v. The following lemmas hold according to the analysis presented in [30]:

Lemma 1. *If*

$$d \leq \sqrt[k]{\frac{a_1}{a_2(1-2^{1-k})}},$$

direct transmission is the most energy-efficient way to deliver packets from u to v.

Lemma 2. *If*

$$d > \sqrt[k]{\frac{a_1}{a_2(1-2^{1-k})}},$$

$\xi(d)$ is minimized when all hop distances are equal to $\frac{d}{N}$, and the optimal number of hops is $\lfloor \frac{d}{d_o} \rfloor$ or $\lceil \frac{d}{d_o} \rceil$, where

$$d_o = \sqrt[k]{\frac{a_1}{a_2(k-1)}}.$$

Lemma 3. *The total energy consumption for delivering 1 bit data over distance d satisfies $\xi(d) \geq a_1 \cdot \frac{k}{k-1} \cdot \frac{d}{d_o}$.*

From Lemma 2, it can be observed that d_o is the optimal forwarding distance in terms of minimizing $\xi(d)$ when d is an integral multiple of d_o. Even if d cannot be divided exactly by d_o, d_o is also a good approximation of the optimal forwarding distance. Moreover, d_o remains constant for given sensor device and application environment since d_o only depends on a_1, a_2, and k. Thus, d_o can act as an effective metric to guide localized packet forwarding to provide energy-efficient routing. Based on this observation, in our study, the ideal next-hop relay position for any node u in terms of minimizing the total energy consumption for delivering a packet from node u to the sink is defined as follows:

Definition 1. *Given any node u, the ideal position of its next-hop relay, denoted by f_u, is defined as the point on the straight line from u to the sink s, where $|uf_u| = d_o$.*

In our scheme, each node makes fully localized and stateless forwarding decisions based on the location of its ideal next-hop relay position.

4 Energy-Efficient Beaconless Geographic Routing (EBGR)

EBGR works in two modes: *beaconless greedy forwarding mode* and *beaconless recovery mode*. In the former mode, only the nodes in the *relay search region* (see Fig. 1) of the forwarder are candidates for further forwarding the packet, and the forwarder chooses the neighbor closest to its optimal relay position as its next-hop relay using the RTS/CTS handshaking mechanism. In this way, each packet is expected to be delivered along the minimum energy route from the source to the sink. If there is no node in the relay search region, the forwarder enters into beaconless recovery mode,

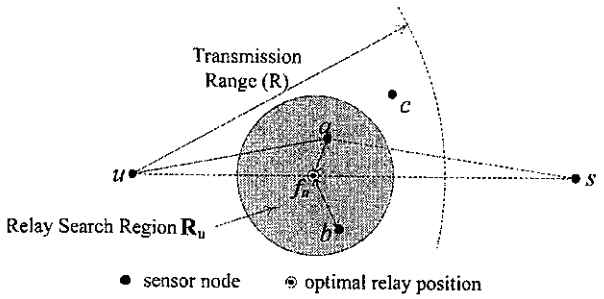

Fig. 1. Greedy forwarding in EBGR.

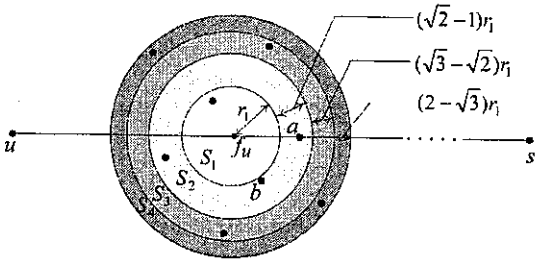

Fig. 2. The relay search region $\mathbf{R}_u$ is divided into four coronas S_1, S_2, S_3, S_4, where S_i has width $(\sqrt{i}-\sqrt{i-1})r_1$ since all coronas have the same area size.

and the beaconless angular relaying is employed to recover from the local minimum.

4.1 Relay Search Region

Since the best next-hop relay for any node u is the neighbor closest to its ideal relay position f_u, there is no need for all neighbors of node u to participate in the contention for acting as the next-hop relay. In EBGR, each node has a relay search region which is defined as follows:

Definition 2. *Given any node u, its next-hop relay search region, denoted by $\mathbf{R}_u$, is defined as the disk centered at u's ideal next-hop relay position f_u with radius $r_s(u)$ where $r_s(u) \leq |uf_u| = d_o$.*

For any node u, only the neighbors in its relay search region $\mathbf{R}_u$ are candidates for further forwarding the packets transmitted from node u. The concept of relay search region is introduced to prohibit the unsuitable neighbors from participating the relay contention procedure.

4.2 Beaconless Greedy Forwarding

Given any node u, let $|us|$ be the distance from node u to the sink s. Node u first calculates $|us|$ since it has the knowledge of its own position as well as the position of the sink. If the sink is in u's transmission range and

$$|us| \leq \sqrt[k]{\frac{a_1}{a_2(1-2^{1-k})}},$$

node u transmits its packets directly to the sink because relaying the packets by some intermediate nodes is no more energy-efficient than direct transmission (see Lemma 1). Otherwise, node u detects it best next-hop relay based on the procedure given as follows:

Let (x_u, y_u) and (x_s, y_s) be the coordinates of node u and the sink s, respectively. By Definition 1, the location of f_u, denoted by (x_{uo}, y_{uo}), can be computed as follows:

$$\begin{cases} x_{uo} = x_u - \dfrac{d_o}{|us|}(x_u - x_s), \\ y_{uo} = y_u - \dfrac{d_o}{|us|}(y_u - y_s). \end{cases}$$

When node u has a packet to transmit, it broadcasts an RTS message, which also contains the location of its ideal next-hop relay position as well as the radius of its relay search region, to detect its best next-hop relay. For any neighbor w that receives the RTS message from node u, it first checks if it falls in $\mathbf{R}_u$. If $w \notin \mathbf{R}_u$, the RTS message is simply discarded. Otherwise, node w generates a CTS message which also contains its own location and sets a proper delay, denoted by $\delta_{w \to u}$, for broadcasting the CTS message based on a discrete delay function given in next section. If node w overhears a CTS message broadcasted by another candidate before $\delta_{w \to u}$ is due, node w cancels broadcasting its own CTS message; otherwise, node w broadcasts its CTS message when $\delta_{w \to u}$ is due. When node u receives the CTS message from its neighbor w, the next-hop relay for u, denoted by $relay(u)$, is updated if $relay(u)$ is null or $|wf_u| < |relay(u)f_u|$. Finally, node w unicasts its packet to its next-hop relay $relay(u)$.

4.3 Discrete Delay Function

In EBGR, the selection of the next-hop relay is performed by means of contention through RTS/CTS handshaking. To reduce the communication overhead incurred by relay selection, a discrete delay function is designed to promote the best relay and suppress the broadcasting of CTS message by other unsuitable neighbors.

For any node u, its relay search region $\mathbf{R}_u$ is divided into n concentric coronas $S_1, S_2 \ldots S_n$ where all coronas have the same area size (see Fig. 2). Thus, the width of the ith corona is $(\sqrt{i}-\sqrt{i-1})r_1$, where r_1 is the radius of S_1 and $r_1 = \frac{r_s(u)}{\sqrt{n}}$. If $v \in S_i$, the distance between node v and f_u satisfies that

$$\frac{\sqrt{i-1} \cdot r_s(u)}{\sqrt{n}} \leq |vf_u| < \frac{\sqrt{i} \cdot r_s(u)}{\sqrt{n}}.$$

Therefore, given any node $v \in \mathbf{R}_u$, v must locate in S_m, where

$$m = \left\lfloor \left(\frac{\sqrt{n} \cdot |vf_u|}{r_s(u)} \right)^2 \right\rfloor + 1.$$

For any node $v \in \mathbf{R}_u$, instead of broadcasting the CTS message immediately after receiving an RTS message from node u, node v broadcasts its CTS message with delay $\delta_{v \to u}$. Let γ be the delay for transmitting a packet over a unit distance. $\delta_{v \to u}$ is defined as follows:

$$\delta_{v \to u} = \frac{\gamma \cdot r_s(u)}{\sqrt{n}} \cdot \left(2 \sum_{i=1}^{m} \sqrt{i} - \sqrt{m} - 1 \right) + \gamma \cdot \left(|vf_u| - \sqrt{\frac{m-1}{n}} r_s(u) \right), \quad (2)$$

where $m = \lfloor (\frac{\sqrt{n}\cdot|vf_u|}{r_s(u)})^2 \rfloor + 1$. The delay computed by (2) guarantees:

1. Nodes in S_i broadcast their CTS messages earlier than nodes in S_j, where $j > i$.
2. Given node $v_i \in S_i$ and node $v_j \in S_j (1 \le i < j \le n)$, it must satisfy that $\delta_{v_j \to u} - \delta_{v_i \to u} > \gamma \cdot |v_i v_j|$, which means that v_j can overhear the CTS message broadcasted by v_i and cancels broadcasting its own CTS message before $\delta_{v_j \to u}$ is due.
3. For all nodes located in the same corona S_i, the node closest to f_u broadcasts its CTS message first because the second term $\gamma \cdot (|vf_u| - \frac{(m-1)r_s(u)}{\sqrt{n}})$ in (2) guarantees that the node closer to f_u has a shorter delay.

It seems that for all nodes in the same corona, the node closest to the sink is the best candidate for packet relaying in terms of minimizing sensor-to-sink energy consumption. In the following, we show that it is not true. As shown in Fig. 2, let $(0,0)$, $(28,0)$, $(23,2)$, and $(40,0)$ be the coordinates for node u, a, b, and s, respectively. Then, $|ub|^2 + |bs|^2 = 23^2 + 2^2 + (40-23)^2 + 2^2 = 826$, and $|ua|^2 + |as|^2 = 28^2 + (40-28)^2 = 928$. Obviously, forwarding the packet transmitted by node u through node b is more energy-efficient than through node a although node a is closer to the sink than node b. In our scheme, node b is assigned a shorter delay than node a and broadcasts the CTS message first. Thus, node b becomes the next-hop relay for node u.

If there is only one node in the innermost nonempty corona, the above delay function guarantees that the number of CTS/RTS messages broadcasted for detecting the best relay for u is minimized (only two messages, one CTS message broadcasted by u and one RTS message broadcasted by the neighbor closest to f_u). Even if there are multiple nodes in the innermost nonempty corona, the above delay function can still significantly reduce the number of CTS messages broadcasted because only the nodes in the most inner nonempty corona have the chance to broadcast CTS messages. Based on this delay function, each node can simply use the largest relay search region (i.e., $r_s(u) = d_o$) to cover more candidates since the delay function can effectively suppress unsuitable neighbors in the relay search region to broadcast CTS messages.

4.4 Beaconless Recovery

When node u broadcasts an RTS message to detect its best next-hop relay, it sets its timer to t_{max} and starts the timer. t_{max} is large enough to guarantee that node u can receive the CTS message from the furthest neighbor in $\mathbf{R}_u$ before the timer is expired. If node u receives no CTS message till the timer is expired, it assumes that there is no neighbor in its relay search region. To recover from the local minimum, the beaconless angular relaying proposed in [17] is employed in EBGR. The angular relaying algorithm works in two phases: *selection phase* and *protest phase*. In the selection phase, the forwarder u broadcasts an RTS message to its neighbors, and the neighbors answer with CTS messages in counterclockwise order according to an angular-based delay function. After the first candidate w answers with a valid CTS, the protest phase begins. First, only the nodes in $N_{GG}(v,w)$ (i.e., the Gabriel circle having uw as diameter) are allowed to protest. If a node x protests, it automatically becomes the next-hop relay. After that, only nodes in $N_{GG}(v,x)$ are allowed to protest. Finally, the forwarder sends the packet to the selected (first valid or last protesting) candidate.

5 Theoretical Analysis of EBGR

In this section, we present extensive theoretical analysis for EBGR based on a simplified MAC model without packet loss, the unit disk graph model without failures in greedy forwarding, and uniform node deployment.

5.1 Notations and Definitions

In [24], two terms, *progress* and *advance*, were introduced to distinguish different forwarding rules in geographic routing. Suppose that node u forwards its packets to its neighbor v for relay to the sink s. The *progress*, denoted by $P(u,v)$, is defined as the projected distance of $|uv|$ on the straight line passing through u and s, and the *advance*, denoted by $A(u,v)$, is defined as the difference between $|us|$ and $|vs|$. Therefore,

$$P(u,v) = |uv| cos \angle vus, \tag{3}$$

$$A(u,v) = |us| - |vs|. \tag{4}$$

We define two metrics called *energy over progress ratio* and *energy over advance ratio* to analyze the characteristics of energy consumption in EBGR. Let $\gamma_P(u,v)$ and $\gamma_A(u,v)$ be the *energy over progress ratio* and the *energy over advance ratio* for relaying 1 bit data from u to v, respectively. $\gamma_P(u,v)$ and $\gamma_A(u,v)$ are defined as follows:

$$\gamma_P(u,v) = \frac{\varepsilon_{relay}(|uv|)}{P(u,v)} = \frac{a_1 + a_2|uv|^k}{|uv| cos \angle vus}, \tag{5}$$

$$\gamma_A(u,v) = \frac{\varepsilon_{relay}(|uv|)}{A(u,v)} = \frac{a_1 + a_2|uv|^k}{|us| - |vs|}. \tag{6}$$

Without loss of generality, we assume that the maximum transmission range (R) is no less than $2d_o$ since the analysis approach for $R < 2d_o$ is the same.

5.2 Guaranteed Delivery

Theorem 1. *EBGR is loop-free in greedy forwarding mode.*

Proof. Let u be a source node and s be the sink. If s locates in the transmission range of node u and

$$|us| \le \sqrt[k]{\frac{a_1}{a_2(1-2^{1-k})}},$$

node u sends its packets directly to the sink without any relay. The theorem holds in this case.

If

$$|us| > \sqrt[k]{\frac{a_1}{a_2(1-2^{1-k})}},$$

the packets generated by node u may be relayed by some intermediate nodes before arriving at the sink. As shown in Fig. 3, the maximum distance from s to any point in $\mathbf{R}_u$ is $|sb|$. $\forall v_1 \in \mathbf{R}_u$, $|v_1 s| \le |bs| < |us|$ because $r_s(u) \le d_o$

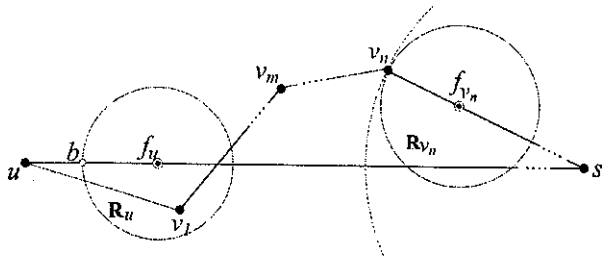

Fig. 3. Illustration of loop-free packet forwarding in greedy forwarding mode.

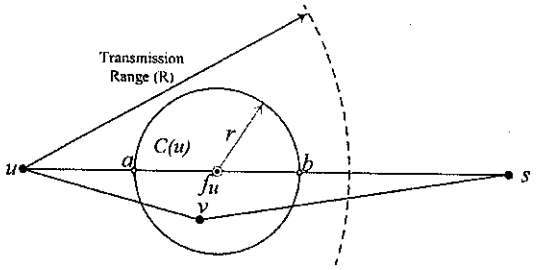

Fig. 4. $C(u)$ is the minimum relay search region that covers only one node and r is the radius of $C(u)$.

and no two nodes locate at the same position. Therefore, $A(u, v_1) = |us| - |v_1 s| > 0$, which means that each forwarding must obtain a positive advance.

Let v_n be a node that relays the packets generated by node u, and $\overrightarrow{v_0 v_1 \ldots v_m \ldots v_{n-1} v_n}$ represents the routing path from u to v_n in EBGR where $v_0 = u$. For any relay node v_m prior to v_n in this routing path, $A(v_n, v_m) = |v_n s| - |v_m s| < 0$, which means that v_n cannot forward its packets to v_n. Hence, the theorem holds. □

By Theorem 1, EBGR is loop-free in beaconless greedy forwarding mode. In beaconless recovery mode, the beaconless angular relaying uses the *Select* and *Protest* methods to avoid crossing edges which might cause a routing loop. In [17], it is proven that the angular relaying algorithm can always select the first edge of the Gabriel subgraph in counterclockwise order. Thus, there are no routing loops in angular relaying. Therefore, EBGR can provide guaranteed delivery as long as the network is connected.

5.3 Bounds on Hop Count

For any node u, let $C(u)$ be the minimum relay search region that covers only one neighbor, and let r be the radius of $C(u)$. Since nodes are uniformly deployed, the minimum relay search regions for all nodes in the network have the same size. Then, we have the following theorem:

Theorem 2. *If there are no failures in greedy forwarding, the number of hops, denoted by N, for delivering a packet from u to the sink s under EBGR where $|us| = d$ satisfies*

$$\frac{d}{d_o + r} - 1 < N < \frac{d}{d_o - r} + 1. \tag{7}$$

Proof. Let v be the node in $C(u)$. As shown in Fig. 4, $|vs|$ is maximized when v locates at point a and minimized when v locates at point b. By (4), $A(u, v) = |us| - |vs|$. Therefore, $d_o - r \le A(u, v) \le d_o + r$.

Let $\overrightarrow{u v_1 v_2 \ldots v_{N-1} s}$ denote the routing path from u to the sink s. Based on (4),

$$\begin{aligned} d &= |us| = A(u, v_1) + |v_1 s| \\ &= A(u, v_1) + A(v_1, v_2) + |v_2 s| \\ &= A(u, v_1) + A(v_1, v_2) + \cdots + A(v_{N-2}, v_{N-1}) + |v_{N-1} s|. \end{aligned}$$

Since $|v_{N-1} s| = A(v_{N-1}, s)$,

$$d = A(u, v_1) + \sum_{i=1}^{N-2} A(v_i, v_{i+1}) + A(v_{N-1}, s).$$

For the prior $N - 1$ hops, the best relay is chosen based on the same metric (i.e., the neighbor closest to the ideal next-hop relay position). Therefore,

$$(N-1)(d_o - r) \le d - A(v_{N-1}, s) \le (N-1)(d_o + r).$$

That is,

$$\begin{aligned} \frac{d - A(v_{N-1}, s) + (d_o + r)}{d_o + r} &\le N \\ &\le \frac{d - A(v_{N-1}, s) + (d_o - r)}{d_o - r}. \end{aligned}$$

For the last hop, the packet is directly transmitted to the sink. Based on Lemma 1,

$$0 < A(v_{N-1}, s) \le \sqrt[k]{\frac{a_1}{a_2(1 - 2^{1-k})}}.$$

By Lemma 8 (see the Appendix), $0 < A(v_{N-1}, s) < 2d_o < 2(d_o + r)$. Thus,

$$\begin{aligned} N &\ge \frac{d - A(v_{N-1}, s) + (d_o + r)}{d_o + r} \\ &> \frac{d - 2(d_o + r) + (d_o + r)}{d_o + r} = \frac{d}{d_o + r} - 1, \end{aligned}$$

and

$$\begin{aligned} N &\le \frac{d - A(v_{N-1}, s) + (d_o - r)}{d_o - r} \\ &< \frac{d + (d_o - r)}{d_o - r} = \frac{d}{d_o - r} + 1. \end{aligned}$$

Therefore,

$$\frac{d}{d_o + r} - 1 < N < \frac{d}{d_o - r} + 1.$$

□

5.4 Upper Bound on Energy Consumption

In EBGR, the best next-hop relay for each node is detected through RTS/CTS handshaking. Since the discrete delay function can effectively suppress unsuitable candidates for broadcasting CTS messages, the number of RTS/CTS messages broadcasted is proportional to the number of hops for delivering the data to the sink. Therefore, the energy consumed by broadcasting and receiving RTS/CTS can be viewed as a part of energy spent by data delivery. In this analysis, the energy consumption for sensor-to-sink

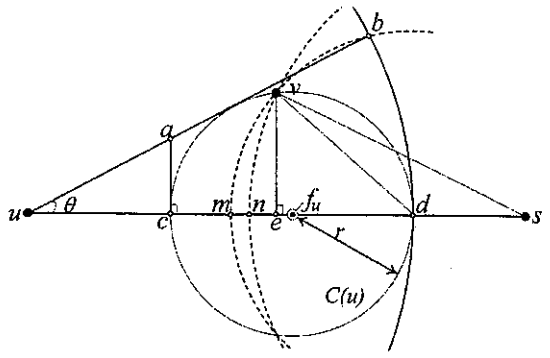

Fig. 5. $C(u)$ is the minimum relay search region and v is a node located on the border of $C(u)$, where $|vs| = |ns|$, $|vd| = |md|$, and $|ud| = |ub|$.

data delivery is referred to as the sum of energy consumed by the nodes in the routing path for delivering 1 bit data from the source to the sink.

In the following, we first prove that the position that maximizes the *energy over advance ratio* $\gamma_A(u,v)$ must be located on the border of the minimum relay search region in Lemma 4. Then, in Lemma 6, we demonstrate that the *energy over advance ratio* at each hop has an upper bound. Finally, the upper bound on energy consumption for sensor-to-sink data delivery is given in Theorem 3.

Lemma 4. *Given $v \in C(u)$, v must locate on the border of $C(u)$ when $\gamma_A(u,v)$ is maximized.*

Proof. Suppose v is located inside $C(u)$. Let v' be a point on the border of $C(u)$ and v' has the same x-coordinate with v. By (6),

$$\gamma_A(u,v') - \gamma_A(u,v) = \frac{\varepsilon_{relay}(|uv'|)}{A(u,v')} - \frac{\varepsilon_{relay}(|uv|)}{A(u,v)} = \frac{a_1 + a_2(|uv'|^k)}{|us| - |v's|} - \frac{a_1 + a_2(|uv|^k)}{|us| - |vs|}.$$

Since $|v's| > |vs|$ and $|uv'| > |uv|$, $\gamma_A(u,v') - \gamma_A(u,v) > 0$. Hence, this lemma holds. □

Lemma 5. *If v locates on the border of $C(u)$ and $r > 0$,*

$$\frac{A(u,v)}{P(u,v)} \geq \frac{r}{d_o + r - \sqrt{d_o^2 - r^2}}.$$

Proof. As shown in Fig. 5, $|vs| = |ns|$ and $|vd| = |md|$. Clearly, $|un| \geq |um|$ because $\angle vns > \angle vms$. By (3) and (4), $\frac{A(u,v)}{P(u,v)} = \frac{|us|-|vs|}{|ue|} = \frac{|us|-|ns|}{|ue|} \geq \frac{|ud|-|md|}{|ue|} = \frac{|ud|-|vd|}{|ue|}$. Assume that u is the origin and the straight line from u to s is the x-axis. $(0,0)$ and (x,y) represent the coordinates of u and v, respectively. Since v locates on the border of $C(u)$, $(x-d_o)^2 + y^2 = r^2$. Thus,

$$\frac{A(u,v)}{P(u,v)} \geq \frac{d_o + r - \sqrt{2r(r+d_o-x)}}{x} \geq \frac{r}{d_o + r - \sqrt{d_o^2 - r^2}}.$$

□

Lemma 6. *Given*

$$v \in C(u), \gamma_A(u,v) < \max\left\{\frac{2a_2 d_o^k\left[k-1+\left(\frac{d_o-r}{d_o+r}\right)\right]}{(d_o-r)\left(1+\sqrt{\frac{d_o-r}{d_o+r}}\right)}, \frac{2a_2 d_o[(k-1)d_o^k + (d_o+r)^k]}{(d_o+r)\left(\sqrt{d_o^2-r^2}+d_o-r\right)}\right\}.$$

Proof. From Lemma 4, v must locate on the border of $C(u)$ when $\gamma_A(u,v)$ is maximized. By (6) and Lemma 5,

$$\gamma_A(u,v) = \frac{a_1 + a_2|uv|^k}{A(u,v)} = \frac{a_1 + a_2|uv|^k}{P(u,v)\frac{A(u,v)}{P(u,v)}} = \gamma_P(u,v)\frac{P(u,v)}{A(u,v)}.$$

Thus,

$$\gamma_A(u,v) \leq \gamma_P(u,v)\frac{d_o + r - \sqrt{d_o^2 - r^2}}{r}.$$

Let $\overline{ub}$ be the tangent of the circle centered at f_u with radius r (see Fig. 5). a and b are two points on the line segment from a to b where $|ua| = (d_o - r)\sec\theta$ and $|ub| = d_o + r$. Let ψ denote the set of points located on the line segment between a and b. $\forall w \in \psi$,

$$\gamma_P(u,w) = \frac{a_1 + a_2|uw|^k}{P(u,w)} = \frac{1}{\cos\theta}\cdot\frac{a_1 + a_2|uw|^k}{|uw|}, \quad (8)$$

where $(d_o - r)\sec\theta \leq |uw| \leq d_o + r$. Clearly, $\gamma_P(u,w)$ given in (8) is strictly concave with respect to $|uw|$. Therefore,

$$\max_{w\in\psi}\gamma_P(u,w) = \max\{\gamma_P(u,a), \gamma_P(u,b)\}. \quad (9)$$

Similar to the proof of Lemma 4, it is easy to prove that $\gamma_P(u,v) \leq \max_{w\in\psi}\gamma_P(u,w)$. By Lemma 5 and (9),

$$\gamma_A(u,v) < \max\{\gamma_P(u,a), \gamma_P(u,b)\} \cdot \frac{d_o + r - \sqrt{d_o^2 - r^2}}{r}, \quad (10)$$

where

$$\gamma_P(u,a) = \frac{a_1 + a_2 d_o^k\left(\frac{d_o-r}{d_o+r}\right)^{\frac{k}{2}}}{d_o - r}$$

and

$$\gamma_P(u,b) = \frac{d_o(a_1 + a_2(d_o+r)^k)}{(d_o+r)\sqrt{d_o^2-r^2}}.$$

By Lemma 2, $d_o = k\sqrt{\frac{a_1}{a_2(k-1)}}$. Replacing $\gamma_P(u,a)$ and $\gamma_P(u,b)$ in (10),

$$\gamma_A(u,v) < \max\left\{\frac{2a_2 d_o^k\left[k-1+\left(\frac{d_o-r}{d_o+r}\right)\right]}{(d_o-r)\left(1+\sqrt{\frac{d_o-r}{d_o+r}}\right)}, \frac{2a_2 d_o[(k-1)d_o^k + (d_o+r)^k]}{(d_o+r)\left(\sqrt{d_o^2-r^2}+d_o-r\right)}\right\}.$$

□

Theorem 3. *If there are no failures in greedy forwarding and no packet loss in EBGR, the total energy consumption, denoted by $\xi(d)$, for delivering 1 bit data from source u to the sink s under EBGR where $|us| = d$ satisfies*

$$\xi(d) < \max\left\{ \frac{2a_2 d_o^k\left[k-1+\left(\frac{d_o-r}{d_o+r}\right)\right]}{(d_o-r)\left(1+\sqrt{\frac{d_o-r}{d_o+r}}\right)}, \frac{2a_2 d_o\left[(k-1)d_o^k+(d_o+r)^k\right]}{(d_o+r)\left(\sqrt{d_o^2-r^2}+d_o-r\right)} \right\} \cdot d.$$

Proof. Let $\xi'(d)$ and N' be the total energy consumption and the number of hops, respectively, for delivering 1 bit data for u to the sink s when all hops including the last one use the same metric (i.e., the neighbor closest to the ideal next-hop relay position) to choose relay. Let d_i denote the distance for the ith hop. Let A_i and $\gamma(i)$ denote the advance and the energy over advance ratio for the ith hop, respectively:

$$\xi'(d) = \underbrace{a_{11}+a_2 d_1^k}_{u} + \underbrace{\sum_{i=2}^{N'} \varepsilon_{relay}(d_i)}_{relay} + \underbrace{a_{12}}_{s}$$
$$= \sum_{i=1}^{N'} \varepsilon_{relay}(d_i) = \sum_{i=1}^{N'} \gamma(i)\cdot A_i.$$

Since all hops are independent and use the same routing metric, $\xi'(d)$ is maximized when the packet is forwarded to the neighbor with the maximum energy over advance ratio at each forwarding. By Lemma 1, $\xi(d) < \xi'(d)$ because the metric used for the last forwarding in EBGR saves energy. Therefore,

$$\xi(d) < \xi'(d) < \left(\max_{i=1}^{N'} \gamma(i)\right) \cdot \sum_{i=1}^{N'} A_i.$$

Based on the proof of Theorem 2, $\sum_{i=1}^{N'} A_i = d$. Thus,

$$\xi(d) < d \cdot \max_{i=1}^{N'} \gamma(i).$$

By Lemma 6, the upper bound on energy over advance ratio only depends on a_2, d_o, k, and r. So, all hops have the same upper bound on energy over advance ratio. Therefore,

$$\xi(d) < \max\left\{ \frac{2a_2 d_o^k\left[k-1+\left(\frac{d_o-r}{d_o+r}\right)\right]}{(d_o-r)\left(1+\sqrt{\frac{d_o-r}{d_o+r}}\right)}, \frac{2a_2 d_o\left[(k-1)d_o^k+(d_o+r)^k\right]}{(d_o+r)\left(\sqrt{d_o^2-r^2}+d_o-r\right)} \right\} \cdot d.$$

□

Let r_{ul} denote the ratio of the upper bound to the lower bound on energy consumption for delivering 1 bit data over distance d in EBGR. We have the following corollary:

Corollary 1.

$$r_{ul} < \max\left\{ \frac{k-1+\left(\frac{d_o-r}{d_o+r}\right)^{\frac{k}{2}}}{k\left(1-\frac{r}{d_o}\right)\sqrt{\frac{d_o-r}{d_o+r}}}, \frac{k-1+\left(1+\frac{r}{d_o}\right)^k}{k\left(1-\frac{r^2}{d_o^2}\right)} \right\}.$$

When $a_{11} = a_{12} = 50\ nJ/bit$, $a_2 = 100\ pJ/bit/m^2$, and

$$k = 2, r_{ul} < \frac{1{,}000}{(\sqrt{1{,}000}-r)(\sqrt{1{,}000-r^2})}.$$

Proof. The proof of this corollary is given in the Appendix. □

From Corollary 1, it is worth noting that $r_{ul} \to 1$ when $r \to 0$. However, r_{ul} becomes infinite when r approaches d_o. This phenomenon can be explained as follows: when r approaches to d_o, as can be been seen in Fig. 5, the advance obtained by forwarding the data to the next-hop relay is very small if the next-hop relay is located at the position closest to node u. Thus, $\gamma_A(u,v)$ must be very large since the energy spent by electronic circuit (i.e., a_{11} and a_{12}) becomes the dominant part in the total energy consumption. Obviously, the worst case is that the next-hop relay for each forwarding node is located at the position that maximizes the energy over advance ratio. Let $Prob_w(d)$ denote the probability that the worst case happens for delivering packets from u to the sink s where $|us| = d$. The following theorem shows that $Prob_w(d)$ approaches to 0 when r approaches to d_o:

Theorem 4. *$Prob_w(d)$ monotonically decreases with the increase of d and r. $Prob_w(d) \to 0$ when $r \to d_o$.*

Proof. Let N be the number of hops for delivering a packet from u to s where $|us| = d$. Let $p(i)$ denote the probability that the packet is forwarded in the way that the energy over advance ratio at hop i is maximized. For the prior $N-1$ hops, the forwarding at each hop is the same and independent. Thus, $p(i) = p(j) \equiv p(1 \le i, j \le N-1)$. We have

$$Prob_w(d) = p(N) \cdot \prod_{i=1}^{N-1} p(i) < p^{N-1}.$$

Since nodes are deployed with uniform distribution, $p \propto \frac{1}{\pi r^2}$. For the hop count N, it increases with the increase of d. Therefore, $Prob_w(d)$ monotonically decreases with the increase of d and r.

From (6), the location that maximizes $\gamma_A(u,v)$ approaches to u when $r \to d_o$ because the advance obtained for each forwarding is very small and a_1 becomes the dominant part in energy consumption. When $r \to d_o$, $N \to \infty$. Therefore, $Prob_w(d) \to 0$ when $r \to d_o$. □

5.5 Expected Energy Consumption

Let $E[\gamma_A(u,v)]$ denote the expected energy over advance ratio for one hop forwarding in EBGR. We have the following lemma:

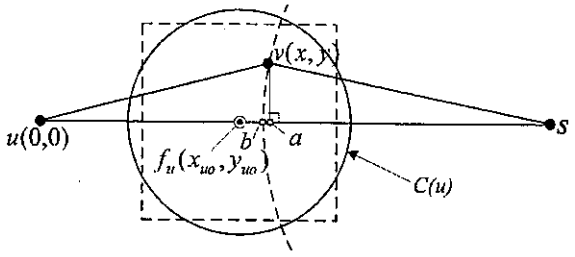

Fig. 6. Approximation of advance where v is the only node in $C(u)$ and $|vs| = |bs|$.

Lemma 7.

$$E[\gamma_A(u,v)] \approx \rho \int\int_{C(u)} \frac{a_1 + a_2(x^2+y^2)^{\frac{k}{2}}}{x} dxdy, \qquad (11)$$

where ρ is the node deployment density.

Proof. Let v be the node in $C(u)$. Since sensor nodes are uniformly distributed with density ρ, by (6),

$$E[\gamma_A(u,v)] = \int\int_{C(u)} \frac{\varepsilon_{relay}(|uv|)}{A(u,v)} \rho dxdy$$
$$= \rho \int\int_{C(u)} \frac{a_1 + a_2|uv|^k}{|us| - |vs|} dxdy.$$

When nodes are densely deployed, $C(u)$ is small. As shown in Fig. 6, the advance obtained by forwarding the packet to v is close to the progress, that is, $|us| - |vs| \approx |ua|$. Thus,

$$E[\gamma_A(u,v)] \approx \rho \int\int_{C(u)} \frac{a_1 + a_2|uv|^k}{|ua|} dxdy$$
$$\approx \rho \int\int_{C(u)} \frac{a_1 + a_2(x^2+y^2)^{k/2}}{x} dxdy. \qquad (12)$$

□

Theorem 5. *If there are no failures in greedy forwarding and no packet loss, the expected energy consumption, denoted by $E[\xi(d)]$, for delivering 1 bit data from source u to the sink s where $|us| = d$ satisfies*

$$E[\xi(d)] \approx \rho d \int\int_{C(u)} \frac{a_1 + a_2(x^2+y^2)^{\frac{k}{2}}}{x} dxdy.$$

Proof. Let N be the number of hops to deliver one packet from u to s. By Lemma 7, it is easy to see that the approximation of $E[\gamma_A(u,v)]$ only depends on ρ. Therefore, the prior $N-1$ hops have the same approximated energy over advance ratio, denoted by $E[\gamma]$, due to the same forwarding procedure. Let $E[\gamma(N)]$ be the energy over advance ratio for the last hop. As shown in Fig. 6,

$$E[\gamma(N)] = \rho \int\int_{C(u)} \frac{a_1 + a_2(|sv|)^k}{|sv|} dxdy.$$

When nodes are densely deployed, $C(u)$ is small and $E[\gamma(N)] \approx E[\gamma]$. Furthermore, the effect of the last hop on the total energy consumption is small for large d. Therefore,

$$E[\xi(d)] = E\left[\sum_{i=1}^{N} \gamma(i) d_i\right] \approx E[\gamma] d$$
$$\approx \rho d \int\int_{C(u)} \frac{a_1 + a_2(x^2+y^2)^{k/2}}{x} dxdy.$$

□

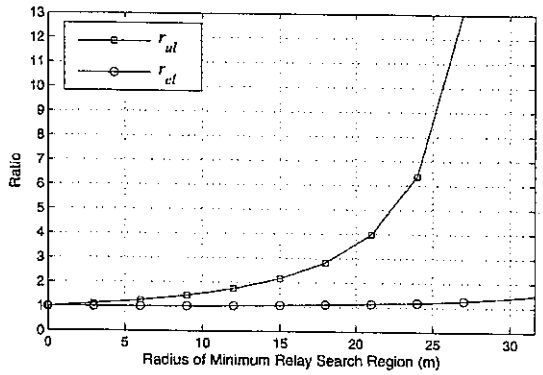

Fig. 7. Comparison of r_{ul} and r_{el} with the variation of the radius of the minimum relay search region.

Let r_{el} be the ratio of the approximated expected energy consumption to the lower bound on energy consumption for delivering 1 bit data from a node to the sink. We have the following corollary:

Corollary 2.

$$r_{el} = \frac{1}{2} + \frac{12d_o^2 + \pi r^2}{24\sqrt{\pi} r d_o} \ln \frac{2d_o + \sqrt{\pi} r}{2d_o - \sqrt{\pi} r} \quad \text{when} \quad k = 2$$

and $r_{el} < 1.5$ when $a_{11} = a_{12} = 50\, nJ/bit$ and $a_2 = 100\, pJ/bit/m^2$.

Proof. The proof of this corollary is given in the Appendix. □

5.6 Summary of Analysis on Energy Consumption

To demonstrate the energy efficiency of EBGR, we give the comparison between r_{ul} and r_{el}. Similar with [3], [14], the system parameters are set as follows: $k = 2$, $a_{11} = a_{12} = 50\, nJ/bit$, and $a_2 = 100\, pJ/bit/m^2$. Under this setting, the optimal hop distance is $\sqrt{1{,}000}$ m according to Lemma 2. The maximum transmission range R for all nodes is set to 80 m which is larger than $2d_o$. Fig. 7 plots r_{ul} and r_{el} under different size of the relay search region. It can be seen that r_{ul} is close to 1 when r is small because a small r means that the best relay for each node keeps very close to its ideal next-hop relay position. With the increase of r, r_{ul} first increases slightly and reaches around 2 when $r = 15$ m. After that, r_{ul} increases quickly with the increase of r and approaches to infinity when r comes near to $\sqrt{1{,}000}$ m. However, r_{el} increases slowly with the increase of r. Even if $r = \sqrt{1{,}000}$ m, r_{el} is less than 1.5. This is because the probability that packets are delivered along the worst path decreases with the increase of r.

6 Extension to Lossy Wireless Sensor Networks

The protocol design and theoretical analysis discussed in the previous sections are based on the UDG model in which transmissions between any two nodes within the communication range are assumed to be reliable. In this section, we extend EBGR to lossy sensor networks to provide energy-efficient sensor-to-sink routing in the presence of unreliable communication links.

6.1 Routing Metric

To capture the characteristics of data loss, *packet reception rate (PRR)* is used to measure the quality of communication links. Let $PRR(u,v)$ be the packet reception rate for link (u,v). $PRR(u,v)$ is defined as the ratio of the number of successful transmissions from u to v to the total number of transmissions from u to v. Thus, the expected number of transmissions that guarantees one successful transmission from u to v is $\frac{1}{PRR(u,v)}$.

Packets may be lost due to many reasons such as data corruption, collision, or the attenuation of signal strength. In the case where a packet is lost before reaching the receiver, nearly the same amount of energy is dissipated by listening [34]. Therefore, the total expected energy consumption for successfully relaying 1 bit data from u to v, denoted by $E[\varepsilon(u,v)]$, can be approximately modeled as

$$E[\varepsilon(u,v)] \simeq \frac{\varepsilon_{relay}(|uv|)}{PRR(u,v)}.$$

By (6), the expected energy over advance ratio, denoted by $E[\gamma_A(u,v)]$, for successfully relaying 1 bit data from u to v satisfies

$$\begin{aligned} E[\gamma_A(u,v)] &\simeq \frac{\varepsilon_{relay}(|uv|)}{PRR(u,v)A(u,v)} \\ &\simeq \frac{1}{PRR(u,v)} \cdot \frac{\varepsilon_{relay}(|uv|)}{A(u,v)}. \end{aligned} \tag{13}$$

Note that the second part $(\frac{\varepsilon_{relay}(|uv|)}{A(u,v)})$ in (13) is the energy over advance ratio when transmission from u to v is reliable. Motivated by this observation, we propose a new metric for providing energy-efficient routing in lossy sensor networks. Instead of choosing the neighbor closest to the ideal next-hop relay position among all candidates in the relay search region, node u chooses the neighbor that minimizes $\frac{|vf_u|}{PRR(u,v)}$ as its next-hop relay. We refer to the extended version of EBGR using this routing metric as EBGR-2.

6.2 Blacklisting and Discrete Delay Function

Blacklisting has been shown as an efficient mechanism to avoid "weak links" [27]. For any node $v \in \mathbf{R}_u$, node v is blacklisted from participating in the contention for acting as packet relay for node u if $PRR(u,v) < \eta$. Let $B(u)$ be the set of remaining nodes in $\mathbf{R}_u$ after blacklisting. Clearly, $\max_{v \in B(u)} \frac{|vf_u|}{PRR(u,v)} \leq \frac{r_s(u)}{\eta}$. A *Discrete Delay Function* similar to the one in EBGR is then used to reduce the number of CTS messages broadcasted. The principle of this discrete delay function is the same with that in EBGR. The nodes in $B(u)$ are divided into n sets $S_1, S_2, \ldots S_n$ based on the following rule: If $v \in S_i$, $\frac{(i-1)\cdot r_s(u)}{\eta} \leq \frac{|vf_u|}{PRR(u,v)} < \frac{i\cdot r_s(u)}{\eta}$. The delay for node v to broadcast its CTS message after receiving an RTS message from u, denoted by $\delta_{v\to u}$, is defined as follows:

$$\delta_{v\to u} = 2(m-1)\cdot\gamma\cdot r_s(u) + \gamma\cdot\frac{|vf_u|}{PRR(u,v)}, \tag{14}$$

where $m = \lfloor \frac{n\cdot\eta\cdot|vf_u|}{r_s(u)\cdot PRR(u,v)} \rfloor + 1$. The delay setting ensures that the neighbors in S_1 broadcast the CTS messages first. Within each set, the neighbor that has a smaller $\frac{|vf_u|}{PRR(u,v)}$ is assigned with a shorter delay. Furthermore, the CTS message broadcasted by a node in one set can be snooped by the nodes in other sets before they broadcast their own CTS messages. It is easy to see that the number of messages needed to be broadcasted is minimized when there is only one node in innermost nonempty set.

7 Simulation Results and Analysis

7.1 Simulation Settings

To study the behavior of EBGR and EBGR-2, we have implemented a simulation package based on OMNeT++ version 3.3 [1]. In all simulations, 200 sensor nodes are randomly deployed in a $500\,m \times 400\,m$ region. Unless specially noted, the only sink is placed at the center of the region. Three scenarios are designed to evaluate the performance of the proposed schemes.

- **Mobility scenario**: All sensor nodes move according to the Random Walk Mobility Model [26]. A sensor node moves from its current location to a new location by randomly choosing a speed from range $[minspeed, maxspeed]$ and a direction from range $[0, 2\pi]$. Each movement continues for an interval of 10 seconds. New speed and direction are chosen at the end of each interval.
- **Random sleeping scenario**: All nodes remain static after deployment, and the Random-Independent Sleeping (RIS) scheme [20] is employed to extend network lifetime. The simulation time is divided into intervals with length of $\mathcal{T}_{sleep}$. At the beginning of each interval, each node decides to work in *active* state with probability p and enter into *sleep* state with probability $1-p$. With this sleeping scheme, the expected network lifetime can be increased by a factor close to $1/p$.
- **High-variant link quality scenario**: All nodes remain static and no sleeping scheme is employed. However, the link quality changes dynamically over time. The behavior of each link is modeled according to a realistic channel model proposed in [7]. The simulation time is divided into link quality estimation intervals with length of $\mathcal{T}_{esti}$. At the end of each interval, each node estimates the PRR of a link from a neighbor to itself by counting the number of beacon or RTS/CTS messages received from that neighbor.

For performance analysis, in addition to EBGR and EBGR-2, we have implemented another three routing schemes: GPER [33], BLR [15], and $PRR \times DIST$ [27]. GPER is a beacon-based geographic routing scheme. Based

on the maintained neighbor information, each node first chooses its neighbor closest to the sink as a subdestination, and then, uses a shortest-path algorithm to compute the energy-optimal next-hop relay. BLR is a beaconless geographic routing scheme based on hop-count routing metric. In all simulations done in this section, the *closest-to-destination* routing metric, in which each node chooses its neighbor closest to the sink as its next-hop relay, is employed in BLR. The $PRR \times DIST$ routing metric is introduced to provide energy-efficient geographic routing in the presence of unreliable transmissions. For each neighbor that is closer to the destination, the product of the reception rate and the distance improvement achieved by forwarding to this neighbor is computed, and the neighbor with the highest value is chosen as the next-hop relay.

The underlying MAC protocol is IEEE 802.11, and the configuration of the MAC protocol is described as follows: For beacon-based schemes (i.e., GPER and $PRR \times DIST$), the RTS/CTS exchange function is turned off to reduce communication overhead since RTS/CTS handshaking is not necessary for these two schemes. For fair comparison, both BLR and EBGR use the RTS/CTS handshaking for selecting the next-hop relay, avoiding packet duplication and reducing packet collisions. In all simulations, the maximum transmission range for each node is set to 80 m. The beacon message is set to 20 bytes. The RTS message is 25 bytes and the CTS message is 20 bytes. For the parameter settings in the delay function of EGBR and EBGR-2, the number of coronas/sets (i.e., n) is set to 20, and the transmission delay (i.e., λ) is 10^{-6} s/m. The radius of the relay search region for each node is set to the largest (i.e., $d_o = \sqrt{1{,}000}\ m$). The recovery timers for both EBGR, EBGR-2, and BLR are set to 40 ms. For the energy model, the energy spent by transmitter electronics on transmitting or receiving 1 bit data (i.e., a_{11} and a_{12}) is set to 50 nJ/bit, the transmitting amplifier (a_2) is set to 10 $pJ/bit/m^2$, and the propagation loss exponent (k) is set to 2.

In each simulation run, 20 nodes are selected as sources and each source generates 40 data packets with a payload of 128 bytes. The simulation is terminated until the sink receives all the data packets generated in the network, and the simulation results are the average of 50 independent runs.

7.2 Energy Consumption for Sensor-to-Sink Data Delivery

In this set of simulations, the sink is placed at the top-left corner of the simulation region, and there is only source which is placed at the bottom-right corner. We measure the total energy consumption for delivering a packet from the source to the sink under different routing schemes, and compare with the theoretical results we obtained. As can be seen from Fig. 8, EBGR consumes nearly the same energy as the optimal routing scheme in which the routing path from the source to the sink in obtained by running Dijkstra's algorithm. With the increase of node deployment density, the energy consumption under EBGR approaches to the lower bound, demonstrating the energy efficiency of EBGR. It is also worth noting that the energy consumption under EBGR keeps close to the expected energy consumption although the upper bound keeps large. Therefore, the expected energy consumption is a good estimation on energy consumption for sensor-to-sink data delivery under EBGR.

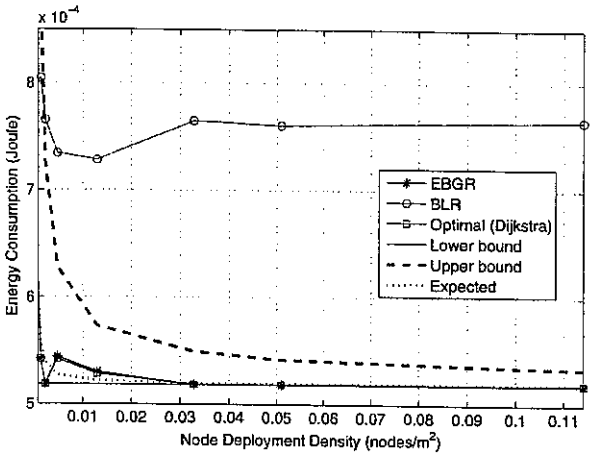

Fig. 8. Energy consumption for sensor-to-sink data delivery with different node deployment density.

7.3 Performance of EBGR in Mobility Scenarios

In this set of simulations, we evaluate the performance of EBGR in mobile scenarios in which the network topology changes frequently due to node mobility. The parameters of the Random Walk Mobility Model are set as follows: *minspeed* is set to 0 m/s, and *maxspeed* is varied from 0 to 50 m/s to provide different levels of mobility. The simulated beacon intervals for GPER are 0.5, 1.0, and 2.0 seconds.

Fig. 9a shows the total energy consumption of GPER, BLR, and EBGR under different mobility levels. The total energy consumption is referred to as the sum of the energy spent by each node in the network during the simulation time. As can be seen from Fig. 9a, EBGR and BLR are much more robust to network topology changes than GPER since each forwarding decision in EBGR and BLR is made based on the actual topology at the time the packet is transmitted. With the increase of *maxspeed*, the energy consumption under EBGR and BLR only increases slightly due to the suboptimal power routes (see Fig. 9d) and slight packet drops (see Fig. 9b) caused by node movement. From Fig. 9b, we can observe that the data packet drop ratios in EBGR and BLR are close to 0. As the maximum movement speed increases, the data packet drop ratio in BLR is a little larger than that in EBGR because each node in BLR tends to choose the neighbor close to the border of the transmission range as its next-hop relay, and it is possible that the established next relay moves out of the transmission range before receiving the data packet.

In contrast, node movement has a great impact on the performance GPER. When *maxspeed* is lower than 5 m/s, GPER with a beacon interval of 2.0 seconds consumes less energy than EBGR because of the low packet drop rate (as shown in Fig. 9b) and the low beacon message overhead (as shown in Fig. 9c). As the maximum movement speed increases, the total energy consumption under GPER increases abruptly. With a maximum movement speed of 50 m/s, GPER with a beacon interval of 0.5 and 1 s consumes 109 and 65 percent more energy than EBGR. This phenomenon can be explained as follows: in scenarios with high node movement speed, the maintained information in GPER becomes outdated quickly, resulting in

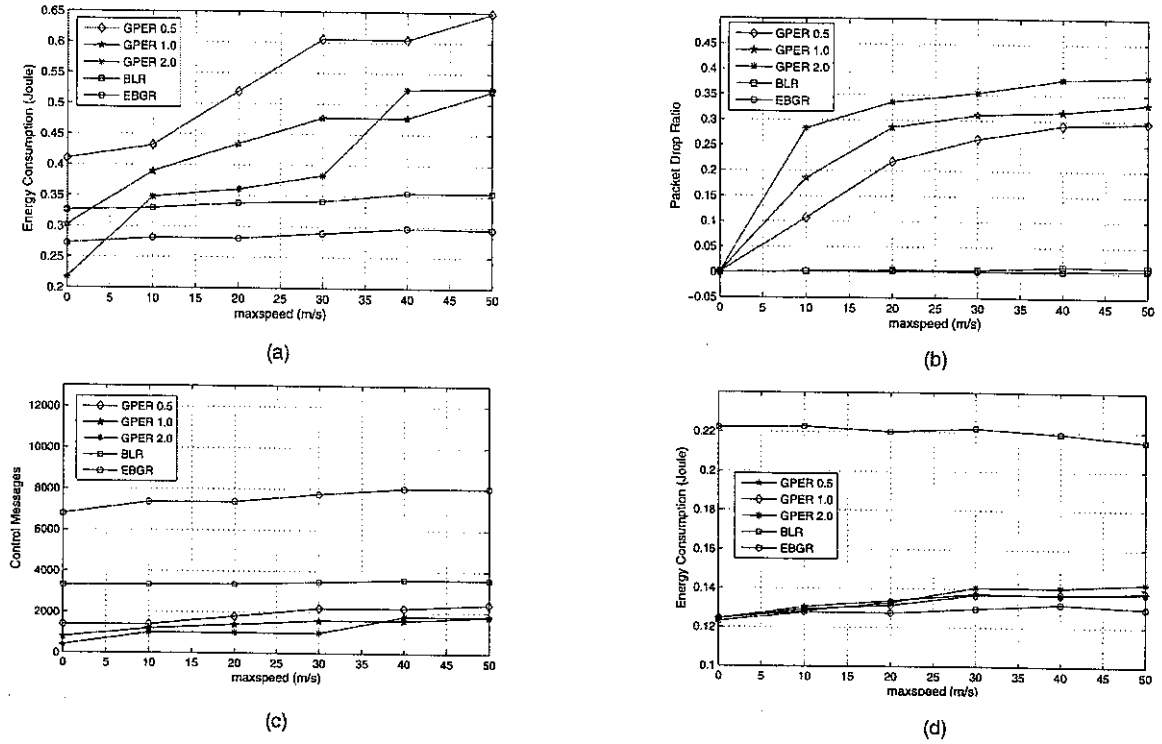

Fig. 9. Performance of EBGR, BLR, and GPER in mobility scenarios with different mobility levels. (a) Energy consumption. (b) Data packet drop Ratio. (c) Control message overhead. (d) Sum of energy consumption along routing path.

frequent packet drops. As shown in Fig. 9b, with a maximum movement speed of 50 m/s, the packet drop ratio can be as high as 0.38 for GPER with a beacon interval of 2 seconds. To provide guaranteed packet delivery, dropped packets must be retransmitted, resulting in much energy wastage. Moreover, frequent packet drops lead to a long sensor-to-sink data delivery delay. Since the number of beacon messages broadcasted in GPER scales proportionally to the running time, much additional energy is consumed by exchanging beacon messages.

It is worth noting that EBGR consumes much less energy than BLR. This result can be explained as follows: First, in BLR, each node chooses its neighbor closest to the sink as its next-hop relay. The hop distance is much larger than the optimal forwarding distance d_o when each node has a large maximum transmission range, resulting in significant energy dissipation since energy consumption on data transmission is proportional to a square of the transmission distance. Fig. 9d shows the sum of energy spent on successful data packet transmission (the energy wasted by unsuccessful packet transmission is not taken into account in order to demonstrate the quality of routing path). It can be seen that BLR consumes at least 80 percent more energy than EBGR, which means that the routing paths in BLR are not energy-efficient. Second, in BLR, the power level for broadcasting RTS message must be large enough so that all nodes in the transmission range of the transmitter can receive the RTS message, whereas in EBGR, the power level for broadcasting RTS message only needs to guarantee that all neighbors in the relay search region can receive the RTS message. The power level for broadcasting RTS message is much smaller than that in BLR with a large maximum transmission range. Fig. 9c shows that the number of RTS/CTS messages broadcasted in BLR is 50 percent less than that in EBGR since the number of RTS/CTS messages is proportional to the number of hops. However, it doesn't mean that the energy spend by broadcasting RTS/CTS messages in BLR must be smaller than EBGR because each node spends more energy to broadcast RTS/CTS messages in BLR.

7.4 Performance of EBGR in Random Sleeping Scenarios

The simulated protocols are slightly modified in order to integrate with the RIS sleeping scheme. For GPER, instead of using a constant beacon interval, each node broadcasts a beacon message only when it switches between *active* and *sleep* states since there is no need to broadcast beacon message if its work status does not change. For EBGR and BLR, a node that has data to transmit broadcasts an RTS message only when it works in *active* state and its remaining active time is large enough to finish forwarding one data packet. A neighbor node can join in the relay contention process only when its remaining active time is large enough to receive the data if it is selected as the next-hop relay.

Fig. 10a shows the energy consumption under EBGR, BLR, and GPER with different sleeping probability where the length of the time interval in RIS is set to 4 seconds. When node sleeping probability is smaller than 0.36, GPER outperforms EBGR and BLR because most of nodes work in active state and the amount of beacon messages broadcasted is small due to the low frequency of states switching. With the increase of node sleeping probability, the energy consumption under GPER increases. There is a peak at $p = 0.5$ due to the high frequency for state switching. When node sleeping probability is larger than 0.6, the energy

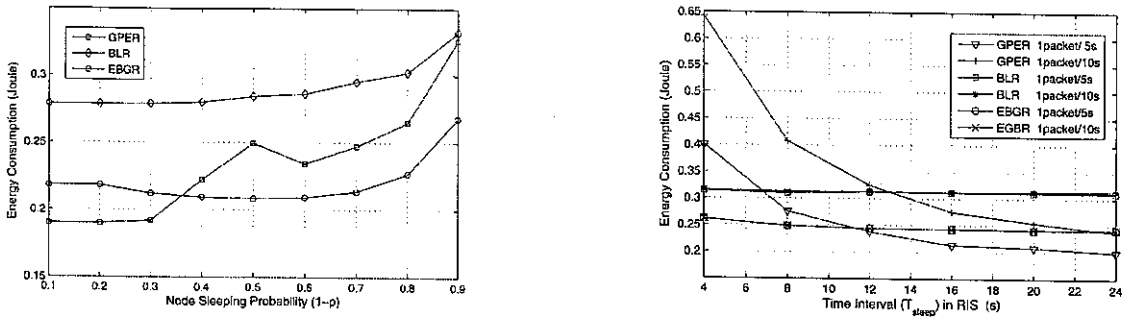

(a) (b)

Fig. 10. Performance of EBGR, BLR, and GPER in random sleeping scenarios with different sleeping probability and time interval. (a) Energy versus sleeping probability. (b) Energy versus time interval in RIS.

consumption for all three protocols increases with the increase of node sleeping probability. The higher the node sleeping probability is, the smaller the number of active nodes is. Thus, nodes with data to transmit switch to recovery mode frequently, resulting in much energy consumption. Moreover, GPER cannot avoid temporary loops although it can prevent infinite loops, which also leads to energy wastage since it is possible that a given packet reaches the same node more than once in GPER.

The size of time interval (i.e., T_{sleep}) in RIS has a great impact on the performance of GPER. Fig. 10b shows the energy consumption under different intervals where node sleeping probability is set to 0.4, and the simulated packet generation rates are 1 $packet/5$ s and 1 $packet/10$ s. It can be seen that EBGR and BLR are independent of the size of T_{sleep} since the next-hop relay for each forwarder is detected in an online manner, and the number of data packets and RTS/CTS messages broadcasted for sensor-to-sink data delivery is proportional to the number of hops. For GPER, packet forwarding is based on the maintained neighbor information. The longer the time interval is, the smaller the amount of beacon messages broadcasted, and the larger the amount of data packets transmitted in one interval. As shown in Fig. 10b, the total energy consumption under GPER decreases with the increase of T_{sleep}. When data generation rate is 1 $packet/5$ s, EBGR outperforms GPER when T_{sleep} is less than 11 s. With the further increase of time interval, GPER consumes less energy than EBGR since less energy is spent on exchanging beacon messages. It is worth noting that GPER with a low data generation rate consumes much more energy than GPER with a high data generation rate because the running time with a low data generation rate is long and much more beacon messages need to be broadcasted. Thus, in contrast to GPER, EBGR is more suitable for event-detection applications in which data generation rate is very low.

7.5 Performance of EBGR-2 in High-Variant Link Quality Scenarios

In this section, we evaluate the performance of EBGR-2 in scenarios where data transmission experiences frequent loss. The loss behavior for each link is modeled based on a realistic channel model proposed in [7]. In this model, two nodes exhibit full connectivity when the distance between them is below a distance D_1. Nodes are disconnected if they are at least distance D_2 away from each other. In the transitional region between D_1 and D_2, the expected reception rate decreases smoothly with some variation. The packet reception rate for a link that has a distance d is computed as follows:

$$PRR(d) = \begin{cases} 1, & \text{if } d < D_1, \\ \left[\dfrac{D_2 - d}{D_2 - D_1} + X\right]_0^1, & \text{if } D_1 \le d < D_2, \\ 0, & \text{if } d \ge D_2, \end{cases} \quad (15)$$

where $[.]_a^b = \max\{a, \min\{b, .\}\}$ and $X \sim N(0, \sigma)$ being a Gaussian variable with variance σ^2. In our simulations, the parameters of this model are set as follows: $D_1 = 20$, $D_2 = 60$, and $\sigma = 0.3$. To demonstrate the energy efficiency of EBGR-2, we compare EBGR-2 with the $PRR \times DIST$ metric designed for routing in lossy sensor networks.

For the routing scheme based on $PRR \times DIST$ metric, each node broadcasts beacon message to update the packet reception ratio for each link at the end of each link quality assessment interval. Fig. 11a shows the total energy consumption under EBGR-2 and $PRR \times DIST$ with the variation of different link quality assessment interval T_{esti}. With the increase of T_{esti}, the energy consumption under EBGR-2 keeps roughly constant, whereas the energy consumption under $PRR \times DIST$ decreases because the number of beacon messages broadcasted decreases with the increase of T_{esti}. Fig. 11b shows the energy spent on transmitting data packets with different link quality assessment interval. In contrast, $PRR \times DIST$ consumes much more energy than EBGR-2. In $PRR \times DIST$, each node chooses its neighbor that maximizes the product of PRR and $DIST$ as its next-hop relay. Thus, each node tends to choose the neighbor with a large hop distance as its next-hop relay, whereas a large hop distance means a large amount of energy consumption for each packet forwarding. As shown in Fig. 11b, $PRR \times DIST$ consumes around 88 percent more energy on data transmission than EBGR-2.

8 Conclusion

Providing energy-efficient routing is an important issue in the design of WSNs. In this paper, we propose a novel energy-efficient beaconless geographic routing protocol EBGR which takes advantages of both geographic routing and power-aware routing to provide loop-free, stateless, and energy-efficient sensor-to-sink routing in dynamic WSNs. The performance of EBGR is evaluated through

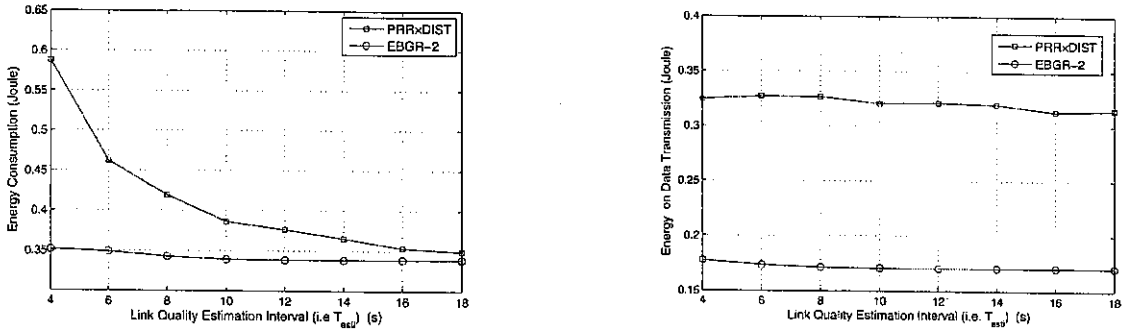

Fig. 11. Performance of EBGR-2 and $PRR \times DIST$ in scenarios with high-variant link quality. (a) Total energy consumption versus link quality estimation interval. (b) Energy on data transmission versus link quality estimation interval.

both theoretical analysis and simulations. We establish the bounds on hop count and the upper bound on energy consumption under EBGR for sensor-to-sink data delivery, assuming no packet loss and no failures in greedy forwarding. Furthermore, we demonstrate that the approximated expected energy consumption under EBGR keeps close to the lower bound when sensor nodes are densely deployed. To deal with the unreliable communication links in WSNs, we extend EBGR to provide energy-efficient routing in lossy sensor networks. Simulation results show that our protocol consumes significantly less energy than routing protocols based on neighborhood maintenance in highly dynamic scenarios.

There are some interesting future research directions regarding the concept of energy-efficient geographical routing in WSNs. By taking the residual energy into account for making forwarding decision, our scheme can be extended to alleviate the unbalanced energy consumption in the network while still guarantee that the total energy consumption for sensor-to-sink data delivery is bounded. Another extension is to integrate other energy-conserving schemes such as data aggregation to further reduce energy consumption and maximize network lifetime. It is also interesting to extend our scheme to networks with heterogeneous propagation properties.

APPENDIX

Lemma 8. $d_o < \sqrt[k]{\frac{a_1}{a_2(1-2^{1-k})}} < 2d_o$, when $k \geq 2$.

Proof. Let

$$f(k) = \frac{\sqrt[k]{\frac{a_1}{a_2(1-2^{1-k})}}}{\sqrt[k]{\frac{a_1}{a_2(k-1)}}} = \sqrt[k]{\frac{k-1}{1-2^{1-k}}} = \sqrt[k]{2^k\left(\frac{k-1}{2^k-2}\right)}.$$

When $k \geq 2$, $1-2^{1-k} < k-1 < 2^k-2$. Thus, $1 < f(k) < k\sqrt{2^k = 2}$. By Lemma 1,

$$d_o = \sqrt[k]{\frac{a_1}{a_2(k-1)}}.$$

Therefore, $d_o < \sqrt[k]{\frac{a_1}{a_2(1-2^{1-k})}} < 2d_o$. □

Proof of Corollary 1:

Proof. By Lemma 3 and Theorem 3, we have

$$r_{ul} < \max\left\{ \frac{2a_2 d_o^k\left[k-1+\left(\frac{d_o-r}{d_o+r}\right)\right]\cdot d}{a_1\cdot\frac{k}{k-1}\cdot\frac{d}{d_o}\cdot(d_o-r)\left(1+\sqrt{\frac{d_o-r}{d_o+r}}\right)}, \right.$$
$$\left. \frac{2a_2 d_o\left[(k-1)d_o^k+(d_o+r)^k\right]\cdot d}{a_1\cdot\frac{k}{k-1}\cdot\frac{d}{d_o}\cdot(d_o+r)\left(\sqrt{d_o^2-r^2}+d_o-r\right)} \right\}.$$

By Lemma 2, $d_o = \sqrt[k]{\frac{a_1}{a_2(k-1)}}$. Replacing d_o with $\sqrt[k]{\frac{a_1}{a_2(k-1)}}$,

$$r_{ul} < \max\left\{ \frac{k-1+\left(\frac{d_o-r}{d_o+r}\right)^{\frac{k}{2}}}{\frac{k}{2}\sqrt{\frac{d_o-r}{d_o+r}}\left(1-\frac{r}{d_o}+\sqrt{1-\frac{r^2}{d_o^2}}\right)}, \right.$$
$$\left. \frac{k-1+\left(1+\frac{r}{d_o}\right)^k}{\frac{k}{2}\left(1+\frac{r}{d_o}\right)\left(1-\frac{r}{d_o}+\sqrt{1-\frac{r^2}{d_o^2}}\right)} \right\}.$$

Since

$$1-\frac{r}{d_o} < \sqrt{1-\frac{r^2}{d_o^2}}, r_{ul}$$
$$< \max\left\{ \frac{k-1+\left(\frac{d_o-r}{d_o+r}\right)^{\frac{k}{2}}}{k\left(1-\frac{r}{d_o}\right)\sqrt{\frac{d_o-r}{d_o+r}}}, \frac{k-1+\left(1+\frac{r}{d_o}\right)^k}{k\left(1-\frac{r^2}{d_o^2}\right)} \right\}.$$

When $a_{11} = a_{12} = 50\ nJ/bit$, $a_2 = 100\ pJ/bit/m^2$, and $k = 2$, by Lemma 2, $d_o = \sqrt{\frac{a_1}{a_2}} = \sqrt{1{,}000}$. Thus, $r_{ul} < \frac{1{,}000}{(\sqrt{1{,}000}-r)(\sqrt{1{,}000-r^2})}$. □

Proof of Corollary 2:

Proof. As shown in Fig. 6, a square centered at f_u with side l is used to approximate $C(u)$ where $l^2 = \pi r^2$. Since $C(u)$ is the minimum relay search region, $\rho\pi r^2 = 1$, that is, $\rho = \frac{1}{\pi r^2}$. When $k = 2$,

$$E[\xi(d)] \approx \frac{d}{\pi r^2}\int_{d_o-l}^{d_o+l}\int_{-l}^{l}\frac{a_1+a_2(x^2+y^2)}{x}dxdy$$
$$\approx \frac{a_2 d(12d_o^2+\pi r^2)}{12\sqrt{\pi}r}\ln\frac{2d_o+\sqrt{\pi}r}{2d_o-\sqrt{\pi}r}+a_2 d d_o. \quad (16)$$

By (16) and Lemma 3,

$$r_{el} = \frac{1}{2} + \frac{12d_o^2 + \pi r^2}{24\sqrt{\pi} r d_o} \ln \frac{2d_o + \sqrt{\pi} r}{2d_o - \sqrt{\pi} r}, \quad \text{where} \quad 0 < r \leq d_o.$$

When $a_{11} = a_{12} = 50\ nJ/bit$, $a_2 = 100\ pJ/bit/m^2$, and $k = 2$, by Lemma 2, $d_o = \sqrt{\frac{a_1}{a_2}} = \sqrt{1{,}000}$. When $r \to 0$, $r_{el} \to 1$. When $r = \sqrt{1{,}000}$, $r_{el} < 1.5$. □

Main symbols Used in this paper:

Symbol	Description
R	maximum transmission range
$\|uv\|$	Euclidean distance between u and v
a_{11}	energy spent by transmitter electronics for transmitting one bit data
a_{12}	energy spent by receiver electronics for receiving one bit data
a_1	$a_{11} + a_{12}$
a_2	transmitting amplifier
k	propagation loss exponent
$\varepsilon_t(x)$	energy spent by transmitting one bit data over distance x
ε_r	energy spent by receiving one bit data
$\varepsilon_{relay}(x)$	energy spent by relaying one bit data
$\xi(d)$	total energy spent on delivering one bit data from u to v where $\|uv\| = d$
d_o	energy optimal hop distance ($\sqrt[k]{\frac{a_1}{a_2(k-1)}}$)
f_u	ideal relay position of node u
$\mathbf{R}_u$	relay research region of node u
$r_s(u)$	radius of $\mathbf{R}_u$
(x_u, y_u)	geographic location of node u
$relay(u)$	next-hop relay of node u
n	number of coronas(or sets) the relay search region is divided into
S_i	i^{th} concentric ring in the relay search region
γ	delay for transmitting a packet over a unit distance
$\delta_{v->u}$	delay for node v to broadcast a reply message to node u
t_{max}	timer for modes switching between greedy forwarding and recovery
$P(u,v)$	progress of node u by forwarding its packets to node v
$A(u,v)$	advance of node u by forwarding its packets to node v
$\gamma_{P(u,v)}$	energy over progress ratio
$\gamma_{A(u,v)}$	energy over advance ratio
$C(u)$	minimum relay search region of node u that covers only one node
r	radius of $C(u)$
N	number of hops in the routing path
ρ	node distribution density
r_{ul}	ratio of upper bound to lower bound on energy consumption
$Prob_w(d)$	probability of worst case for delivery packets over distance d
r_{el}	ratio of approximated expected energy consumption to the lower bound
$PRR(u,v)$	packet reception rate for link (u,v)
η	threshold for blacklisting
T_{sleep}	time interval in random sleeping scheme
p	node sleeping probability in random sleeping scheme
T_{esti}	link quality estimation interval

ACKNOWLEDGMENTS

This work is partially supported by Australian Research Council Discovery Project grant #DP0985063. Haibo Zhang was with the School of Computer Science at The University of Adelaide, Australia. The corresponding author is Hong Shen.

REFERENCES

[1] http://www.omnetpp.org/index.php, 2009.
[2] L. Barrière, P. Fraigniaud, L. Narayanan, and J. Opatrny, "Robust Position-Based Routing in Wireless Ad Hoc Networks with Irregular Transmission Ranges," *Wireless Comm. and Mobile Computing*, vol. 3, pp. 141-153, 2003.
[3] M. Bhardwaj and A.P. Chandrakasan, "Bounding the Lifetime of Sensor Networks via Optimal Role Assignments," *Proc. IEEE INFOCOM*, pp. 1587-1596, 2002.
[4] M. Bhardwaj, T. Garnett, and A.P. Chandrakasan, "Upper Bounds on the Lifetime of Sensor Networks," *Proc. IEEE Int'l Conf. Comm. (ICC)*, pp. 785-790, 2001.
[5] B. Blum, T. He, S. Son, and J. Stankovic, "IGF: A State-Free Robust Communication Protocol for Wireless Sensor Networks," Technical Report CS-2003-11, Univ. of Virginia, 2003.
[6] H.T.K.B. Karp, "GPSR: Greedy Perimeter Stateless Routing for Wireless Networks," *Proc. ACM MobiCom*, pp. 243-254, 2000.
[7] M. Busse, T. Haenselmann, and W. Effelsberg, "Energy-Efficient Forwarding Schemes for Wireless Sensor Networks," *Proc. Int'l Symp. World of Wireless, Mobile and Multimedia Networks (WoWMoM)*, pp. 125-133, 2006
[8] J.-H. Chang and L. Tassiulas, "Maximum Lifetime Routing in Wireless Sensor Networks," *IEEE/ACM Trans. Networking*, vol. 12, no. 4, pp. 609-619, Aug. 2004.
[9] M. Chawla, N. Goel, K. Kalaichelvan, A. Nayak, and I. Stojmenovic, "Beaconless Position Based Routing with Guaranteed Delivery for Wireless Ad-Hoc and Sensor Networks," *Proc. FIP Int'l Federation for Information Processing World Computer Congress*, pp. 61-70, 2006.
[10] G.G. Finn, "Routing and Addressing Problems in Large Metropolitan-Scale Internetworks," Technical Report ISI/RR-87-180, 1987.
[11] H. Frey and I. Stojmenovic, "On Delivery Guarantees of Face and Combined Greedy-Face Routing in Ad Hoc and Sensor Networks," *Proc. ACM MobiCom*, pp. 390-401, 2006.
[12] H. Füßler, J. Widmer, M. Käsemann, M. Mauve, and H. Hartenstein, "Contention-Based Forwarding for Mobile Ad Hoc Networks," *Ad Hoc Networks*, vol. 1, pp. 351-369, 2003.
[13] L. Galluccio, A. Leonardi, G. Morabito, and S. Palazzo, "A MAC/Routing Cross-Layer Approach to Geographic Forwarding in Wireless Sensor Networks," *Ad Hoc Networks*, vol. 5, pp. 872-884, 2007.
[14] W.R. Heinzelman, A. Chandrakasan, and H. Balakrishnan, "Energy-Efficient Communication Protocol for Wireless Microsensor Networks," *Proc. 33rd Hawaii Int'l Conf. System Sciences*, pp. 4-7, 2000.
[15] M. Heissenbüttel, T. Braun, T. Bernoulli, and M. Wälchli, "BLR: Beacon-Less Routing Algorithm for Mobile Ad Hoc Networks," *Computer Comm.*, vol. 11, pp. 1076-1086, 2004.
[16] C. Hsin and M. Liu, "Network Coverage Using Low Duty-Cycled Sensors: Random and Coordinated Sleep Algorithms," *Proc. Third Int'l Symp. Information Processing in Sensor Networks (IPSN)*, pp. 433-442, 2004.
[17] H. Kalosha, A. Nayak, S. Rührup, and I. Stojmenovic, "Select-and-Protest-Based Beaconless Georouting with Guaranteed Delivery in Wireless Sensor Networks," *Proc. IEEE INFOCOM*, pp. 346-350, 2008.
[18] K. Kalpakis, K. Dasgupta, and P. Namjoshi, "Efficient Algorithms for Maximum Lifetime Data Gathering and Aggregation in Wireless Sensor Networks," *Computer Networks*, vol. 42, pp. 697-716, 2003.
[19] F. Kuhn, R. Wattenhofer, and A. Zollinger, "Worst-Case Optimal and Average-Case Efficient Geometric Ad-Hoc Routing," *Proc. ACM MobiCom*, pp. 267-278, 2003.
[20] S. Kumar, T.H. Lai, and J. Balogh, "On Kcoverage in a Mostly Sleeping Sensor Network," *Proc. ACM MobiCom*, pp. 144-158, 2004.

[21] J. Kuruvila, A. Nayak, and I. Stojmenovic, "Hop Count Optimal Position Based Packet Routing Algorithms for Ad Hoc Wireless Networks with a Realistic Physical Layer," *Proc. First IEEE Int'l Conf. Mobile Ad-Hoc and Sensor Systems (MASS)*, pp. 398-405, 2004.
[22] S. Lee, B. Bhattacharjee, and S. Banerjee, "Effcient Geographic Routing in Multihop Wireless Networks," *Proc. ACM MobiHoc*, pp. 230-241, 2005.
[23] Q. Li, J. Aslam, and D. Rus, "Distributed Energy-Conserving Routing Protocols for Sensor Network," *Proc. IEEE 36th Hawaii Int'l Conf. System Science*, 2003.
[24] T. Melodia, D. Pompili, and I.F. Akyildiz, "Optimal Local Topology Knowledge for Energy Efficient Geographical Routing in Sensor Networks," *Proc. IEEE INFOCOM*, 2004.
[25] I.S.P. Bose, P. Morin, and J. Urrutia, "Routing with Guaranteed Delivery in Ad Hoc Wireless Networks," *Proc. Third ACM Int'l Workshop Discrete Algorithms and Methods for Mobile Computing and Comm.*, pp. 48-55, 1999.
[26] M. Sanchez and P. Manzoni, "A Java-Based Ad Hoc Networks Simulator," *Proc. SCS Western Multiconf. Web-Based Simulation Track*, 1999.
[27] K. Seada, M. Zuniga, A. Helmy, and B. Krishnamachari, "Energy-Efficient Forwarding Strategies for Geographic Routing in Lossy Wireless Sensor Networks," *Proc. Second Int'l Conf. Embedded Networked Sensor Systems (SenSys)*, pp. 108-121, 2004.
[28] S. Singh, M. Woo, and C.S. Mghavendra, "Power-Aware Routing in Mobile Ad Hoc Networks," *Proc. ACM MobiCom*, pp. 181-190, 1998.
[29] I. Stojmenovic, "Localized Network Layer Protocols in Wireless Sensor Networks Based on Optimizing Cost over Progress Ratio," *IEEE Network*, vol. 20, no. 1, pp. 21-27, Jan./Feb. 2006.
[30] I. Stojmenovic and X. Lin, "Power-Aware Localized Routing in Wireless Networks," *Proc. 14th Int'l Parallel and Distributed Processing Symp. (IPDPS)*, p. 371, 2000.
[31] I. Stojmenovic and X. Lin, "Power-Aware Localized Routing in Wireless Networks," *IEEE Trans. Parallel and Distributed Systems*, vol. 12, no. 11, pp. 1122-1133, Nov. 2001.
[32] H. Takagi and L. Kleinrock, "Optimal Transmission Ranges for Randomly Distributed Packet Radio Terminals," *IEEE Trans. Comm.*, vol. COM-32, no. 3, pp. 246- 257, Mar. 1984.
[33] S. Wu and K.S. Candan, "GPER: Geographic Power Efficient Routing in Sensor Networks," *Proc. IEEE Int'l Conf. Network Protocols (ICNP)*, pp. 161-172, 2004
[34] Y. Xu, J. Heidemann, and D. Estrin, "Geography-Informed Energy Conservation for Ad Hoc Routing," *Proc. ACM MobiCom*, pp. 70-84, 2001.
[35] H. Zhang and H. Shen, "EEGR: Energy-Efficient Geographic Routing in Wireless Sensor Networks," *Proc. IEEE Int'l Conf. Parallel Processing (ICPP)*, 2007.
[36] M. Zorzi, "A New Contention-Based MAC Protocol for Geographic Forwarding in Ad Hoc and Sensor Networks," *Proc. IEEE Int'l Conf. Comm. (ICC)*, pp. 3481-3485, 2004.

Haibo Zhang received the BS and MS degrees in computer science from Shandong Normal University, and the PhD degree from the School of Computer Science at The University of Adelaide. He is currently a postdoctoral researcher in Automatic Control Laboratory, Royal Institute of Technology, Sweden. His research interests include wireless communication and sensor networks.

Hong Shen received the BE degree from Beijing University of Science and Technology, the ME degree from the University of Science and Technology of China, and the PhLic and PhD degrees from Abo Akademi University, Finland, all in computer science. He is a professor (chair) of computer science at The University of Adelaide, Australia, and also a specially appointed professor at the University of Science and Technology of China. He was a professor and the chair of the Computer Networks Laboratory in Japan Advanced Institute of Science and Technology (JAIST) during 2001-2006, and a professor (chair) of computer science at Griffith University, Australia, where he taught nine years since 1992. With main research interests in parallel and distributed computing, algorithms, data mining, high-performance networks, and multimedia systems, he has published more than 200 papers including over 100 papers in international journals such as a variety of the IEEE and ACM transactions. He received many awards/honors including the 1991 National Education Commission Science and Technology Progress Award and the 1992 Chinese Academy of Sciences Natural Sciences Award. He serves on the editorial board of several journals.